Coupling Reactions of End- vs Mid-Functional Polymers

Hyun K. Jeon,*,† Christopher W. Macosko,† Bongjin Moon,‡,⊥ Thomas R. Hoye,‡ and Zhihui Yin§,#

Department of Chemical Engineering and Materials Science and Department of Chemistry, University of Minnesota, Minneapolis, Minnesota 55455, and Center for Education and Research on Macromolecules (CERM), University of Liège, Start-Tilman B6a, 4000 Liège, Belgium

Received December 10, 2003

ABSTRACT: Reactive compatibilization of immiscible polymer blends is typically accomplished by grafting reactions between functional groups distributed randomly on one polymer and end-functional groups on the other polymer. A number of model studies have focused on end coupling in polymer melts. In this work we compare directly reaction rate constants for an end-functional chain reacting with an end-functional chain, k_E, vs reacting with a mid-functional chain, k_M, using competitive reaction of phthalic anhydride end- and mid-functional poly(methyl methacrylate) (PMMA-eAn and PMMA-mAn) with amine terminal PMMA and polystyrene (PMMA-NH_2 and PS-NH_2). PMMA-eAn was labeled with 7-nitrobenz-2-oxa-1,3-diazole (NBD) while PMMA-mAn was labeled with anthracene. We measured the extent of coupling to block and graft copolymers selectively at the characteristic excitation and emission wavelengths of NBD and anthracene using a fluorescence detector coupled with GPC. We found that coupling with the mid-functional PMMA was slower under all reaction conditions investigated and had the increasing order of k_E/k_M: homogeneous melt (1.7), solution (2.8), heterogeneous blend prepared in the mixer (2.6−3.2), and static flat interface (>10). The kinetic excluded-volume effect and steric hindrance due to the polymer chain are considered to be the reasons for $k_E/k_M > 1$ in the homogeneous case. k_E/k_M in solution was in agreement with the value (2.1) predicted by the kinetic excluded-volume theory. The large value of k_E/k_M in the static flat interface was attributed to end-group segregation at the interface. Interestingly, we found that flow affected the interfacial reaction tremendously, resulting in over 1000 times higher rate constant in heterogeneous melt blending than that in the static bilayer film.

Introduction

Ever since Flory proposed the equal reactivity assumption for polymerization,[1] reactions between polymer-bound reactive groups have attracted research interest. Pioneering work by Morawetz et al. proposed that functional groups attached to polymers experience a kinetic excluded-volume effect, that is, shielding by the polymer coils.[2] They found that in a dilute solution of a good solvent the rate constant decreased from that for the small molecule analogues. Moreover, their results suggested that the reactivity depends on the location of the functional group along the polymer chain. Since their work, there have been many experimental efforts to quantify the kinetic excluded-volume effect, but the results are not consistent.[3−8]

Reactions between polymer-bound functional groups in melts rather than solution are of great interest for reactive compatibilization. Recently, reaction kinetics in homogeneous melts were compared with small molecule analogues.[9,10] Ferrari and Baker reported that the reaction rate of aliphatic secondary amine/maleic anhydride slowed when the maleic anhydride moiety was incorporated into the polymer.[9] They explained that this was due to the excluded-volume effect of the polymer backbone adjacent to the reactive anhydride. In contrast, Orr et al. reported that the rate constant between end-functional polymers with various functional group pairs was in agreement with the rate constant for reaction between analogous functional small molecules.[10]

Reaction in an immiscible polymer blend is confined to the interfaces between the components. It is uncertain whether reaction kinetics studied in the homogeneous melt can be applied to heterogeneous interfacial coupling. Guegan et al. compared the rate constant for interfacial coupling between carboxylic acid terminal polystyrene (PS-COOH) and epoxy terminal PS (PS-E) (homogeneous) vs epoxy terminal poly(methyl methacrylate) (PMMA-E) (heterogeneous).[11] They assumed that reaction could only occur in an "interfacial volume" defined by the surface area of the minor phase and an interfacial thickness (∼5 nm). With this assumption the rate constant for the interfacial coupling was twice as large as that of the homogeneous reaction. Moreover, Orr observed that the rate constants of various functional groups in heterogeneous blends ranked in a different order than in homogeneous blends.[12] To understand the characteristics and kinetics of interfacial coupling without any external flow, reactions at flat static interfaces have been investigated.[13−21] It was suggested that external flow in the mixer during polymer blending process accelerated the interfacial coupling rate to a great extent from that of the static flat interface.[22,23] However, there are few direct comparisons between reactions under these two conditions.

In commercial reactive blends, rather than diblock copolymers, graft copolymers are typically formed by the reaction between compatibilizers with functional groups randomly distributed along a chain and end-functional

† Department of Chemical Engineering and Materials Science, University of Minnesota.
‡ Department of Chemistry, University of Minnesota.
§ University of Liège.
⊥ Present address: Department of Chemistry, Sogang University, Shin-Soo Dong 1, Mapogu, Seoul 121-742, South Korea.
Present address: Department of Chemistry, University of Toronto, 80 St. George Street, Toronto, Ontario M5R 3H6, Canada.
* To whom correspondence should be addressed: Tel +1-612-625-0584; Fax +1-612-626-1686; e-mail jeon@cems.umn.edu.

10.1021/ma030581n CCC: $27.50
Published on Web 03/12/2004

Table 1. Characteristics of the Polymers Used

polymer	M_n (kg/mol)	M_w/M_n	functionality	fluorescent group (label)
PS-NH_2[a]	26	1.14	0.85	
PMMA-NH_2[b]	36	1.13	0.50	
PMMA-eAn	15	1.21	~1	NBD
PMMA-mAn	18	1.27	0.90	anthracene
PS[c]	18	1.05		
PMMA	13	1.17		

[a] Synthesized at the University of Liège, Belgium. [b] Obtained from Polymer Source, Montreal Quebec, Canada. [c] Received from the Dow Chemical Co.

polymers like polyamides or polyesters. Other than the contradictory results for the solution reactions reported previously,[3,5,7,8] it seems that there are no systematic studies on the effect of reactive group location along a polymer chain on the reaction rate, especially in polymer melts. In addition, it is even more important to understand how the interface in immiscible polymer blends affects the coupling rate when a functional group is attached to the middle of a chain to form graft copolymer.

In this study, we have investigated the effect of functional group location along a chain on the coupling rate between two complementary functional polymers under various reaction conditions: solution, homogeneous melt, static flat interface, and heterogeneous blend in the mixer. We used phthalic anhydride end- and mid-functional PMMA (PMMA-eAn and PMMA-mAn) fluorescently labeled with 7-nitrobenz-2-oxa-1,3-diazole (NBD) and anthracene, respectively. We examined the competitive couplings with amine terminal PMMA (PMMA-NH_2) and polystyrene (PS-NH_2) for homogeneous and heterogeneous reactions in the melt, respectively. We were able to detect block copolymer formation and graft copolymer formation separately by setting the excitation and emission wavelengths of a fluorescence detector connected to a GPC at the characteristic wavelengths for NBD and anthracene, respectively. By comparing reactions in homogeneous melts and in heterogeneous blends, we explored the effect of the interface on reaction rate. In addition, we studied the effect of flow on interfacial reaction by comparing results from static flat interfaces to heterogeneous blends prepared in a mixer.

Experimental Section

Materials. Characteristics of the polymers used in this study are shown in Table 1, and the chemical structure of the functional groups is shown in Figure 1. Nonfunctional polymers were synthesized by anionic polymerization, and anhydride functional polymers and PS-NH_2 were synthesized by atom transfer radical polymerization (ATRP). PMMA-NH_2 was used as purchased from Polymer Source.

PMMA-eAn and PMMA-mAn were synthesized using di-*tert*-butyl phthalate (DTBP) functionalized ATRP initiators. The initiators were prepared by the Diels−Alder reaction between di-*tert*-butyl acetylenedicarboxylate and myrcene followed by several steps and final α-bromoester installation.[24] PMMA-eAn and PMMA-mAn were fluorescently labeled by copolymerization with 2-[methyl-(7-nitro-2,1,3-benzoxadiazol-4-yl)-amino]hexyl-2-methyl-2-propenoate (NBD-MA) monomer and (9-anthryl)methyl-2-methyl-2-propenoate (anthracene-MMA) monomer, respectively.[25] Molecular weights of the polymers were determined by using GPC based on PS standards, and for determining molecular weights of PMMA, universal calibration was applied. Functionalities of PMMA-eAn and PMMA-mAn were measured by a coupling reaction with 2 mol equiv of PS-NH_2 in dry tetrahydrofuran (THF) for 2 days at room temperature followed by GPC analysis with a fluorescence detector. Amine functionality of PS-NH_2 was determined by measuring the extent of coupling with 2 mol equiv of unlabeled PMMA-eAn (M_n = 21 kg/mol) using a UV detector connected to the GPC. For PMMA-NH_2, we determined the functionality by coupling with excess of PMMA-eAn in melts at 200 °C since we obtained very low functionality (0.11) by reaction in solution. The low functionality in solution might be due to reversible uptake of CO_2 by aliphatic amine to give carbamic acid at room temperature during storage. It is known that heating this carbamic acid recovers amine by removing CO_2.[26,27]

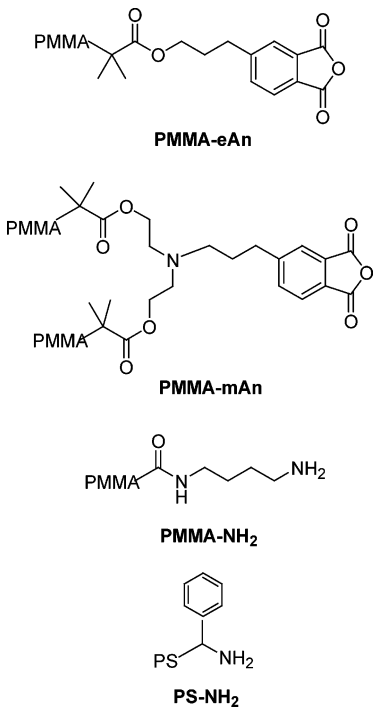

Figure 1. Chemical structure of the functional polymers used in this study.

Reaction Conversion Determinations. Competitive reactions were conducted to obtain the reaction rate constant ratio of PMMA-eAn and PMMA-mAn with amine functional polymers. Amine was the limiting functional group in the reactions with the exception of the reaction at a flat interface. Thus, PMMA-eAn and PMMA-mAn compete with each other to react with the amine terminal polymer. Initial concentration ratios of phthalic anhydrides at the end and at the center and amine groups, $C_{E,0}$:$C_{M,0}$:$C_{A,0}$, for each reaction examined in this study are listed in Tables 2 and 3. The reaction was monitored using GPC with a fluorescence detector after quenching the reaction using THF with 1 vol % phenyl isocyanate. For example, Figure 2 shows the GPC traces obtained for the 90/10 w/w (PMMA + PMMA-eAn + PMMA-mAn)/PS-NH_2 blend after 0.5 min mixing at 180 °C. Only NBD labeled polymers, that is, PMMA-eAn and the reactively formed block copolymer, PMMA-*b*-PS, shown as the thick solid line in the upper curves were detected by setting the excitation and emission wavelengths, λ_{ex} and λ_{em}, at 466 and 539 nm, respectively. To detect anthracene-labeled polymers, PMMA-mAn and the reactively formed graft copolymer, PMMA-*g*-PS (the thick solid line in the lower curves), λ_{ex} and λ_{em} were set at 358 and 402 nm, respectively.

Reaction conversion was measured by a simple peak subtraction method as shown in Figure 2. The dotted lines are for the pure PMMA-eAn and PMMA-mAn, and the thin solid curves are for the corresponding product copolymers after peak subtraction. The peak of pure PMMA-eAn (or PMMA-mAn) was multiplied by a weighting factor and was then subtracted from the bimodal peak of the blend. The weighting factor was changed until a smooth peak of PMMA-*b*-PS (or PMMA-*g*-PS)

Table 2. Rate Constants, k_E and k_M, and Their Ratio, k_E/k_M, for the Homogeneous Reactions

reaction	amine concn,[a] $C_{A,0}$ (mmol/kg)	concn ratio $C_{E,0}$:$C_{M,0}$:$C_{A,0}$	k_E/k_M	k_E (kg/(mol min))	k_M (kg/(mol min))
solution (THF)[b]	0.82	1:1:1	2.8	44	16
		2:0:1		39	
		0:2:1			18
melt at 180 °C[c]	3.50	1.8:1.8:1	1.7	93	55
		1.8:0:1		84	
		0:1.8:1			53
melt at 160 °C[c]	3.50	1.8:1.8:1	1.8	21	12

[a] Concentration based on the total weight of a system. [b] PS-NH_2 was used for the reaction at room temperature. [c] PMMA-NH_2 was used for the melt reactions.

Table 3. Rate Constants k_E and k_E/k_M for the Heterogeneous System Assuming Homogeneous Reactions and $k_{E,I}$ after Considering the Reaction at the Interface

reaction	$C_{A,0}$ (mmol/kg)[a]	$C_{E,0}$:$C_{M,0}$:$C_{A,0}$	k_E/k_M	k_E[b] (kg/(mol min))	D_{VS} (μm) at 2 min	ϕ_I	$k_{E,I}$ (kg/(mol min))
static flat film[c]	22.0	1:1:2.3	~10	0.031		0.0096	3.2
blend-2[d]	0.66	1:1:1	3.2	121	0.13	0.023	5300
blend-10[d]	3.28	1:1:1	2.6	124	<0.05	>0.06	<2100

[a] Concentration based on the total weight of the system. [b] k_E was calculated assuming homogeneous reaction. [c] Reaction temperature was 175 °C. [d] 90/10 PMMA/PS blends at 180 °C. The numbers represent wt % of PS-NH_2 in the blend.

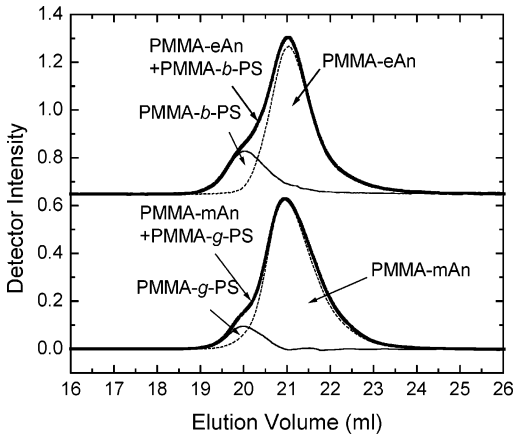

Figure 2. GPC traces obtained for 90/10 w/w (PMMA + PMMA-eAn + PMMA-mAn)/PS−NH_2 blend taken after 0.5 min mixing at 180 °C. Upper and lower thick curves are for NBD and anthracene-labeled polymers, respectively, in the blend. Conversion was measured from the peak area ratio of the copolymer (thin curves) and the blend (thick curves) after subtracting the peak of unreacted PMMA-An (dotted curve) from the peaks of the blend.

with a similar peak shape to the pure PMMA-eAn (or PMMA-mAn) peak was obtained as shown in Figure 2. Fractional conversion of PMMA-eAn (X_E) or PMMA-mAn (X_M) was determined by the area ratio of the copolymer peak to the bimodal peak.

Determination of Rate Constants and Their Ratio. The final product of the cyclic anhydride/amine reaction is an imide, via an amic acid intermediate. While amic acid formation from cyclic anhydride/amine is, in principle, reversible, it is known that for aliphatic amines the reverse reaction can be neglected at ambient temperature.[28] In addition, the subsequent imidization step is very slow at room temperature.[28] Thus, we have ignored the reverse reaction and ring closure for imide formation in the solution reaction and have applied second-order kinetics.

At high temperature, the reaction will proceed to form imide rapidly.[15,28] Using GPC, we are unable to distinguish the imide-linked from amic acid-linked copolymer. Thus, for the melt reactions we also have assumed second-order kinetics. For the heterogeneous melt reaction, we measured the apparent rate constants by assuming a homogeneous reaction.

Competitive second-order reaction is expressed as follows:

$$\begin{aligned} A + E &\xrightarrow{k_E} B \\ A + M &\xrightarrow{k_M} G \end{aligned} \quad (1)$$

where A, E, M, B, and G represent amine, anhydride at the end, anhydride in the middle, reactively formed block copolymer, and graft copolymer, respectively, and k_E and k_M are the rate constants for block and graft copolymers formation, respectively. For this competitive reaction, we write two rate equations for E and M and one mass balance equation.

$$\frac{dX_E}{dt} = k_E C_{A,0}(1 - X_A)(1 - X_E) \quad (2)$$

$$\frac{dX_M}{dt} = k_M C_{A,0}(1 - X_A)(1 - X_M) \quad (3)$$

$$C_{A,0}(1 - X_A) - C_{E,0}(1 - X_E) - C_{M,0}(1 - X_M) = C_{A,0} - C_{E,0} - C_{M,0} \quad (4)$$

By dividing eq 2 by eq 3 and integrating, we obtain eq 5.

$$\frac{k_E}{k_M} = \frac{\ln(1 - X_E)}{\ln(1 - X_M)} \quad (5)$$

Using eqs 4 and 5, we can rewrite eq 2 into eq 6.

$$\frac{dX_E}{dt} = k_E C_{A,0}[M_E(1 - X_E)^2 + M_M(1 - X_E)^a + (1 - M_E - M_M)(1 - X_E)] \quad (6)$$

where $M_E = C_{E,0}/C_{A,0}$, $M_M = C_{M,0}/C_{A,0}$, and $a = k_M/k_E + 1$. Thus, integration of eq 6 gives eq 7.

$$f(X_E) = \int_0^{X_E} \frac{dX_E}{M_E(1 - X_E)^2 + M_M(1 - X_E)^a + (1 - M_E - M_M)(1 - X_E)} = k_E C_{A,0} t \quad (7)$$

The integral function of X_E, $f(X_E)$, is numerically determined at each reaction time and plotted as a function of time. The slope of $f(X_E)$ vs t gives k_E, and k_M is determined by k_E/k_M and k_E.

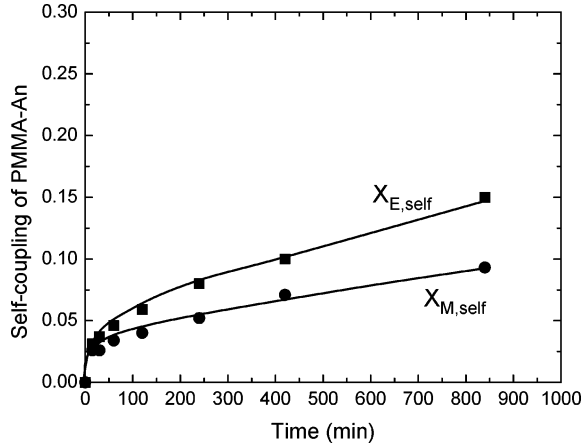

Figure 3. Self-coupling of PMMA-An with annealing time at 175 °C for a bilayer with nonfunctional PS. Filled square and circle are for PMMA-eAn and PMMA-mAn, respectively.

To examine whether the competitive reaction environment affects the rate constants, we carried out the noncompetitive reactions and measured k_E and k_M by eqs 8 and 9.

$$\ln \frac{M_i - X_{A,B(or\ G)}}{M_i[1 - X_{A,B(or\ G)}]} = C_{A,0}(M_i - 1)k_i t \quad (M_i \neq 1) \tag{8}$$

$$\frac{X_{A,B(or\ G)}}{1 - X_{A,B(or\ G)}} = C_{A,0}k_i t \quad (M_i = 1) \tag{9}$$

Here, i = E or M, and $X_{A,B} = M_E X_E$ and $X_{A,G} = M_M X_M$ are the fractional conversions of PS-NH_2 to block (B) and graft (G) copolymer in the noncompetitive reaction, respectively.

Homogeneous Reaction. We first examined the reaction in solution at room temperature. 5 wt % solutions of PS-NH_2 and (PMMA-eAn + PMMA-mAn) in dry THF were prepared separately and then mixed together. Aliquots of solution were taken and quenched with phenyl isocyanate at 1, 5, 10, 20, 40, 60, 120, and 540 min.

Homogeneous melt reaction was carried out using PMMA-NH_2. PMMA-eAn and PMMA-mAn were preblended with PMMA for 1 min prior to the addition of PMMA-NH_2 in a preheated cup-rotor mixer (MiniMax CS-183MMX, Custom Scientific Instrument, Inc.) with three steel balls.[29] The reaction temperature was 180 °C under a N_2 environment. The rotor speed was 340 rpm, which corresponds to 100 s^{-1}. The rotor was lifted at 0.5, 1, 2, 4, 6, 10, and 20 min after adding PMMA-NH_2, and ~10 mg of the blend sample was taken from the edge of the bottom surface of the rotor, followed by freezing it in liquid N_2.

Heterogeneous Reaction: Static. For the reaction at a static interface, a 5 wt % solution of (PMMA-eAn + PMMA-mAn) in toluene was spin-coated on a 3 cm × 3 cm square piece of Si wafer at room temperature. The film thickness (~170 nm) was measured by using a stylus profiler (DektakII, Veeco Inc.). After drying the residual solvent overnight, PS-NH_2 with a thickness of ~350 nm was spin-coated on the (PMMA-eAn + PMMA-mAn) layer from a 5 wt % solution in 87/13 v/v cyclohexane/toluene. After drying the solvent, the square sample was broken into several pieces, and a cover glass was put on top of each piece.[21] The samples were annealed for 15, 30, 60, 120, 240, 420, and 840 min in a vacuum oven at 175 °C. The sample was removed from the vacuum oven at each annealing time. Self-coupling of fluorescently labeled PMMA-An has been reported for flat film samples annealed for long times;[21] thus, we measured the extent of self-coupling after annealing a bilayer with nonfunctional PS for the same time intervals under the same condition. Figure 3 shows the extent of self-coupling with annealing time. Self-coupling at 30 min was about 3% and continued to increase up to 840 min. We subtracted the conversion for self-coupling from the conversion for the bilayer with PS-NH_2.

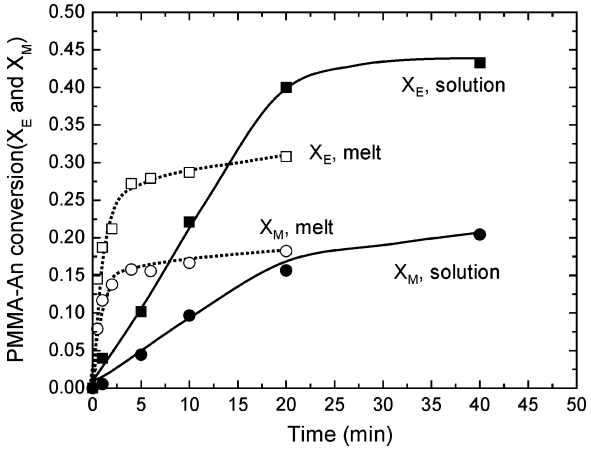

Figure 4. Fractional conversions, X_E (squares) and X_M (circles), of PMMA-eAn and PMMA-mAn to PMMA-*b*-PS and PMMA-*g*-PS, respectively, vs time. Filled and open symbols are for the solution reaction at ambient temperature and the reaction in the homogeneous melt at 180 °C, respectively. Solid and dotted lines are for guiding eyes.

Heterogeneous Reaction: Flow. 90/10 w/w PMMA/PS blends were prepared at 180 °C in the MiniMax Mixer with a N_2 blanket. Weight percents of PS-NH_2 based on the total blend were 2 wt % (blend-2) and 10 wt % (blend-10). Dry-blended PMMA-eAn, PMMA-mAn, and PMMA were pre-blended for 1 min at 180 °C before addition of dry-blended PS and PS-NH_2. Blend samples were taken at 0.5, 1, 2, 4, 6, 10, and 20 min and were quenched in liquid nitrogen. Morphology was observed using transmission electron microscopy (TEM, JEOL 1210) by microtoming the blend specimen to 50 nm thickness at room temperature and then staining with RuO_4 (0.5% aqueous solution) vapor for 20 min. The area of each particle, A_i, was measured using image analysis software (Image Tool, UTHSCSA), and the corresponding diameter was calculated by eq 10. The volume to surface area average particle diameter, D_{VS}, was calculated by eq 11.

$$D_i = 2\left(\frac{A_i}{\pi}\right)^{1/2} \tag{10}$$

$$D_{VS} = \frac{\sum_i D_i^3}{\sum_i D_i^2} \tag{11}$$

Results

Homogeneous Reaction. The filled symbols in Figure 4 represent conversions vs time in solution at ambient temperature. Both X_E and X_M increase linearly up to 20 min, at which about 55% of PS-NH_2 is consumed. After then, conversions increase slowly up to 120 min when the PS-NH_2 is all consumed (not shown in Figure 4). Data before 20 min show that PMMA-*g*-PS formation is slower than PMMA-*b*-PS. To determine k_E/k_M, following eq 5, we plotted $\ln(1 - X_E)$ vs $\ln(1 - X_M)$ using the data obtained before 20 min in Figure 5. The values are tabulated in Table 2. In solution, coupling to PMMA-*b*-PS is 2.8 times as fast as the grafting reaction to PMMA-*g*-PS.

We calculated k_E to be 44 kg/(mol min) from the slope of $f(X_E)$ vs time (<20 min) (Figure 6); accordingly, k_M is 16 kg/(mol min). For comparison, k_E and k_M for the noncompetitive reactions were measured to be 39 and 18 kg/(mol min), respectively, at the same condition with $M_E = M_M = 2$. Fair agreement between the rate constants at these two conditions indicates that the

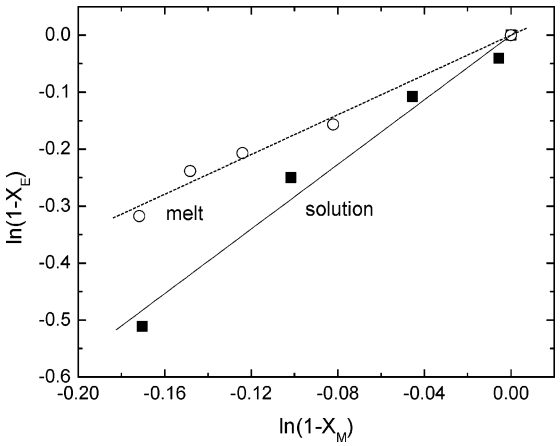

Figure 5. $\ln(1 - X_E)$ vs $\ln(1 - X_M)$ in competitive reaction for the homogeneous case. Filled square and open circle are for the reactions in solution and in the homogeneous melt, respectively. k_E/k_M is the slope of the linearly fitted line shown as the solid for solution and the dotted for homogeneous melt.

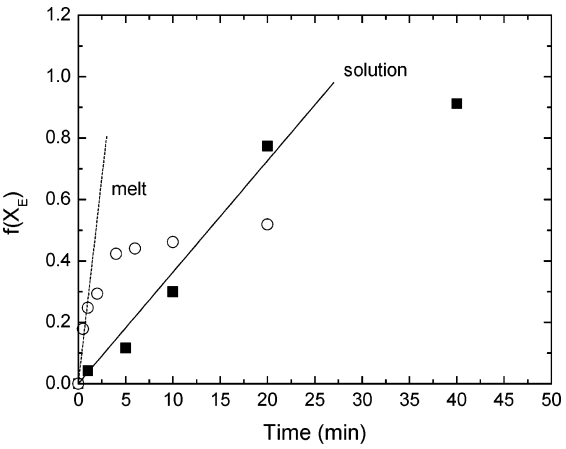

Figure 6. $f(X_E)$ in eq 4 is plotted as a function of time for the homogeneous reactions in solution (filled squares) and in the melt (open circles). The rate constant to block copolymer in the competitive reaction, k_E, was estimated from the initial slope of $f(X_E)$ vs time for each condition.

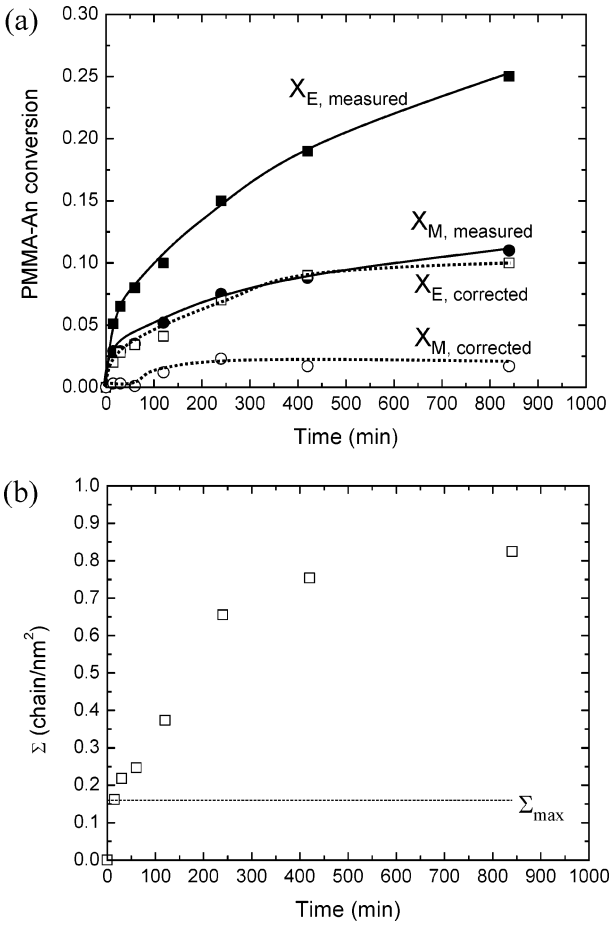

Figure 7. X_E and X_M vs annealing time in the static flat bilayer film of (PMMA-eAn + PMMA-mAn)/PS-NH_2 at 175 °C in (a): $X_{i,\text{measured}}$ (filled symbols) and $X_{i,\text{corrected}}$ (open symbols) are before and after correcting for self-coupling shown in Figure 3, respectively. In (b), interfacial coverage by copolymer, Σ, is plotted as a function of annealing time. For calculation of Σ, the molecular architecture of the copolymer was neglected. The dotted horizontal line represents the maximum coverage, $\Sigma_{max} = 0.16$ chains/nm^2, that is estimated for the lamellar structure of the pure block copolymer.

reaction rate constant measured in the competitive reaction is the inherent value for the PS-NH_2/PMMA-An reaction. However, these are much larger than the value observed by Padwa et al.[28] They reported 0.07 M^{-1} min^{-1} at 30 mM (the concentration of the functional groups in styrene−maleic anhydride copolymer (SMA)/ PS-NH_2 reaction in anisole) at room temperature. A possible cause for this difference is a solvent effect (THF vs anisole) on the reactivity difference between succinic anhydride and phthalic anhydride toward primary amine. According to Padwa et al., the rate constant of the phthalic anhydride/amine reaction is smaller than that of succinic anhydride/amine in anisole.[28] On the contrary, Moon conducted the competitive reaction of phthalic anhydride and succinic anhydride with PS-NH_2 in THF at room temperature, which is the same as our reaction conditions, and found that phthalic anhydride reacted with PS-NH_2 5 times faster than succinic anhydride.[30] These two contrary results imply that the anhydride/amine reaction is sensitive to the reaction environment.

We plotted X_E and X_M vs time for the homogeneous melt reaction at 180 °C (open symbols in Figure 4). Coupling was almost complete in 5 min. As in solution, the PMMA-eAn/PMMA-NH_2 reaction in the melt is faster than the PMMA-mAn/PMMA-NH_2 reaction. The plot of $\ln(1 - X_E)$ vs $\ln(1 - X_M)$ in Figure 5 gives k_E/k_M of 1.7, which is less than the rate ratio (2.8) for the reaction in solution. k_E and k_M in the competitive melt reaction were determined to be 93 and 55 kg/(mol min) at 180 °C by fitting $f(X_E)$ vs time at $t \leq 2$ min, as shown in Figure 6. These were similar to the values from the noncompetitive reactions with $M_E = M_M = 1.8$, where $k_E = 84$ and $k_M = 53$ kg/(mol min). The value of k_E compares reasonably with our previous work, but it is about 1 order of magnitude lower than that for the PS melt reaction.[10] k_E/k_M was 1.8 when we ran the melt reaction at 160 °C (Table 2). This implies that k_E/k_M is not sensitive to temperature change in the melt.

Heterogeneous Reaction: Static. X_E and X_M before and after correction for self-coupling of PMMA-An are shown as a function of annealing time for the reaction at the static interface in Figure 7a. It is evident that the contribution of self-coupling of PMMA-eAn and PMMA-mAn to the measured conversions for the bilayer reaction is significant. During the first 60 min, X_M was not detectable (<0.003) after correction for self-coupling, while X_E increased steadily to 0.03. After 60 min, the

Table 4. Rate Constant, k_E and $k_{E,I}$, Estimated for Previous Studies

	polymer 1/polymer 2 M_{n1}/M_{n2} (kg/mol)	conv (time, min)[a]	k_E (kg/(mol min))	D_{VS} (μm)	ϕ_I	$k_{E,I}$ (kg/(mol min))
static flat film	PS-NH_2/PMMA-An 17/15[b] [18]	0.092 (40)	0.063		0.0054	12
	PS-NH_2/PMMA-An 18/12[c] [21]	0.15 (60)	0.061		0.0042	15
melt mixing	PEE-NH_2/PS-An 18/35[b] [21,47]	0.47 (2)	38	0.2[d]	0.022	1700
	PS-NH_2/PMMA-An (26 + 72)/12[e] [46]	0.35 (0.5)	51	0.14	0.054	950
	PS-NH_2/PMMA-An 15/12[f] [25]	0.43 (2)	64	0.61[g]	0.015	4200

[a] Conversion of limiting polymer, normalized by functionality. The number in parentheses is the time the conversion data were taken. [b] At 200 °C. [c] At 175 °C. For others, temperature = 180 °C. [d] After 20 min. [e] The blend consisted of mixture of 18% 26 kg/mol PS-NH_2, 57% 72 kg/mol PS-NH_2, 10% PMMA-An, and 15% nonfunctional PMMA. [f] PS-NH_2 and PMMA-An were diluted with nonfunctional PS and PMMA to 10% and 8.3% of the blend, respectively. [g] 10 min.

rate of increase in X_E slowed, and X_M became observable.

To determine k_E/k_M for the static interface, we should examine when the interface is saturated with copolymer since it is known that significant undulation of the interface can occur above maximum interfacial coverage, Σ_{max}.[14,18,21,31] Previous studies on similar PS-NH_2/PMMA-An bilayers indicate that spontaneous roughening occurs at about $2\Sigma_{max}$.[32] The interfacial coverage, Σ, for the flat interface of the bilayer film is calculated by eq 12.[21]

$$\Sigma = \frac{X_A t_{PS} \rho_{PS} N_{av}}{M_{n,PS}} \tag{12}$$

Here, t_{PS} is the thickness of the PS-NH_2 layer, ρ_{PS} the density of PS (= 1 g/cm^3), N_{av} Avogadro's number, and $M_{n,PS}$ the molecular weight of PS-NH_2. Figure 7b shows Σ with annealing time. Σ at 15, 30, and 60 min is 0.16, 0.22, and 0.25 chain/nm^2, respectively. For comparison, Σ_{max} for a lamellar structure of the pure diblock copolymer is determined to be 0.16 chains/nm^2 using $\Sigma_{max} = (\lambda/2)N_{av}/(M_{n,c}/\rho)$ and ignoring asymmetry of the copolymer, where λ is the lamellar spacing and $M_{n,c}$ is the molecular weight of block copolymer. The value of λ is estimated to be 22.3 nm.[33,34] In Figure 7b, Σ_{max} is shown as a dotted horizontal line, and spontaneous roughening is expected after 60 min where $\Sigma > 2\Sigma_{max}$. In addition to interfacial roughening, it should be noted that the self-coupling would affect dynamics of polymer chains in the melts and the interface, especially at longer annealing times (>100 min). Thus, k_E/k_M and k_E were determined by using data up to 60 min to exclude the effect of interfacial roughening and change in polymer dynamics by the self-coupling on the reaction rate.

k_E/k_M was roughly estimated to be >10 using X_E = 0.034 at 60 min and X_M = 0.003 (detectable limit). Assuming that the reaction can occur homogeneously throughout the ~ 500 nm thick bilayer gives k_E = 0.031 kg/(mol min) (Table 3). A better assumption is that reaction can only occur in the region where PS and PMMA chains overlap. For PS and PMMA, this interfacial width a_I = 5 nm[33] gives $k_{E,I} = k_E/\phi_I$ = 3.2 kg/(mol min), which is still more than 30 times less than the homogeneous reaction. Here, the interfacial volume fraction, ϕ_I, for the bilayer film is

$$\phi_I = a_I A_V = \frac{a_I}{t} \tag{13}$$

where A_V is the interfacial area per unit volume and t is the bilayer film thickness. For comparison, we estimated $k_{E,I}$ for previous studies on PS-NH_2/PMMA-An bilayers (Table 4).[18,21] $k_{E,I}$ is 12 kg/(mol min) for the PMMA-An (M_n = 15 kg/mol) and PS-NH_2 (M_n = 17 kg/mol) bilayer at 200 °C in Yin et al.'s study.[18] For the bilayer of PMMA-An (M_n = 12 kg/mol) and PS-NH_2 (M_n = 18 kg/mol) at 175 °C reported by Jones et al.,[21] $k_{E,I}$ is roughly estimated to be 14 kg/(mol min) by assuming PS layer thickness of 1 μm. Thus, our $k_{E,I}$ value is in reasonable agreement with the previous data.

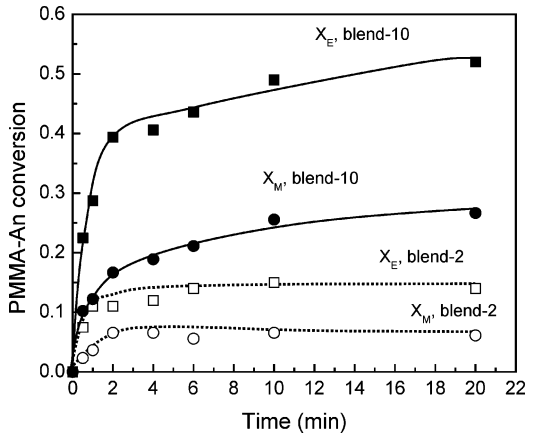

Figure 8. X_E (squares) and X_M (circles) with mixing time for 90/10 w/w (PMMA + PMMA-eAn + PMMA-mAn)/(PS + PS−NH_2) blends at 180 °C. Filled and open symbols are for the blends with 10% PS-NH_2 (blend-10) and 2% PS-NH_2 (blend-2), respectively.

Heterogeneous Reaction: Flow. In contrast to the case of the static interface, the coupling in blend-10 was so fast that 56% of PS-NH_2 converted to copolymer within 2 min of mixing, as shown in Figure 8. After 2 min, the conversions slowly increased until 80% of PS-NH_2 was consumed to form the copolymers at 20 min. When we decreased the amount of PS-NH_2 to 2% (blend-2), the reaction appears to stop after 2 min and 20% overall conversion. Parts a and b of Figure 9 show the morphologies of blend-10 and blend-2 at 20 min mixing, respectively. As expected, in blend-10 most of the reactively formed copolymers form micelles resulting in D_{VS} = 43 nm, while blend-2 exhibits droplets-in-matrix morphology with D_{VS} = 0.26 μm.

We measured k_E/k_M using the data up to 2 min for both blends as shown in Table 3. The interface in the melt-mixed blends reduced k_E/k_M to less than 3.2 from that of the static flat interface, but it is larger than 1.7 measured in the homogeneous melt reaction. It was observed that k_E/k_M increased when we decreased the amount of PS-NH_2 in the blend to 2%. Assuming homogeneous reaction, k_E for both blends was determined by eq 7 and are listed in Table 3. k_E for the blend under flow is about 4000 times larger than that for the static flat interface and is slightly larger than that measured for the homogeneous melt reaction. $k_{E,I}$ was

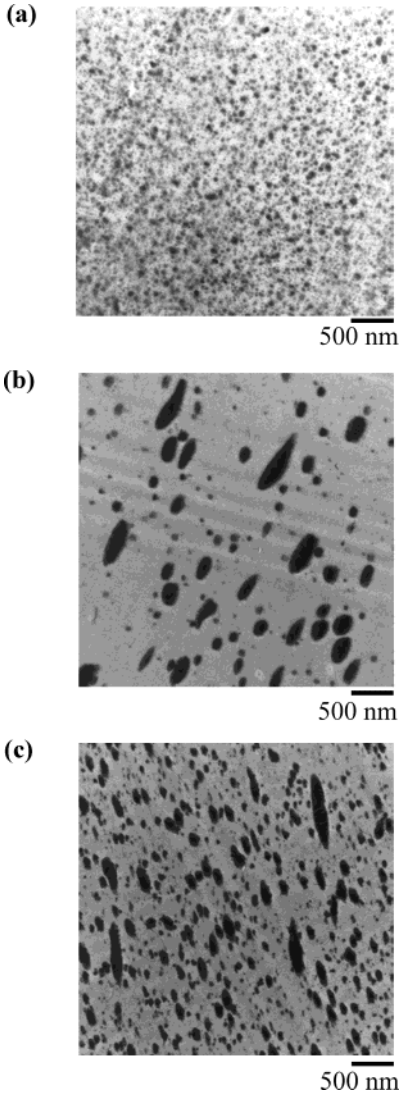

Figure 9. TEM micrographs of (a) blend-10 and (b) blend-2 at 20 min mixing. Morphology at 2 min of blend-2 is shown in (c).

calculated to be 5300 kg/(mol min) for blend-2 using the interfacial volume fraction

$$\phi_I = \frac{6a_I\phi_{PS}}{D_{VS}} \tag{14}$$

where ϕ_{PS} the volume fraction of PS in the blends. D_{VS} was measured for blend-2 after 2 min of mixing (Figure 9c and Table 3). For blend-10, $k_{E,I} < 2100$ kg/(mol min) by assuming that D_{VS} at 2 min <50 nm. We believe that this is because the interface effect under flow has already been reduced due to high conversion. It should be noted that $k_{E,I} > 20k_E$ in the homogeneous reaction. This was not observed in Guégan et al.'s study where $k_{E,I}$ for PS-COOH/PMMA-E was about twice as large as k_E for PS-COOH/PS-E.[11] The difference is considered to be caused by differences in chemistry (amine/anhydride vs epoxy/acid), backbone chemical structure for homogeneous reaction (PMMA vs PS), and/or mixing efficiency of the mixer.

Discussion

According to our results, functional groups at the center of polymer chains experienced greater hindrance reacting with complementary functional polymers than those at the ends in all the reaction conditions examined. The impact of this hindrance as observed by the k_E/k_M rate ratios increased in order from the homogeneous melt, to solution, to the interface in a heterogeneous blend under external flow, to a static flat interface. Estimation of the rate constants revealed that the external flow applied to the heterogeneous blends greatly accelerated the interfacial reaction, giving even higher rate constants than that in the homogeneous reaction.

Homogeneous Reaction. The kinetic excluded-volume effect is anticipated to be significant for a dilute polymer solution in a good solvent.[2,5−7] Theory predicts that the kinetic excluded-volume effect is more pronounced for higher molecular weight polymers and for centrally substituted polymers.[2,35,36]

Khokhlov derived a scaling theory for the kinetic excluded-volume effect on the kinetics of chemical reactions between polymers in dilute solutions.[36] The kinetic excluded-volume effect on the rate constant k is scaled as $(N_1 + N_2)^{-\nu}$, where N_1 and N_2 are degrees of polymerization of polymers 1 and 2, respectively. He categorized the reaction into three cases according to the functional group position along a chain: end and end, end and center, and center and center; the exponent ν is 0.16, 0.28, and 0.43 for each case. Since our reactions are in the first and second categories, $k_E/k_M = (N_1 + N_2)^{0.12}$. Inserting $N_1 = 165$ for PMMA-An, which is the numerical average of N of PMMA-eAn and PMMA-mAn, and $N_2 = 250$ for PS-NH_2, we obtain $k_E/k_M = 2.1$. Our somewhat higher result, 2.8, is most likely due to steric effects as discussed below. The experimental data we find in the literature and comparable with k_E/k_M were reported by Black and Worsfold.[6] They observed that, for the reaction of acid chloride and nitrophenol functional PS in benzene, the rate constant between two end-functional PS was 3.5 times as large as that between two randomly substituted PS with M_n of 70 kg/mol. Khokhlov's scaling theory predicts 7 for the rate ratio of end and end to center and center for $M_n = 70$ kg/mol. We believe that Black and Worsford's lower value is because of random distribution of the functional groups along chains making some groups at the end.

In the melt (or a θ solution) the kinetic excluded-volume effect will be screened and $k_E/k_M = 1$. However, we observed $k_E/k_M = 1.7$ for the reaction between (PMMA-eAn + PMMA-mAn) and PMMA-NH_2 in the melt. Similar results were also observed by Worsfold for interpolymer interaction forming a transition complex.[7] Namely, the kinetic excluded-volume effect decreased in θ solution but did not disappear. This was attributed to the use of mixed solvents and/or oversimplified theories. In our case, there should not be any solvent effect, so we considered some plausible factors that might affect k_E/k_M in the homogeneous melt reaction.

The effect of polymer chain dynamics could be a factor. Welp et al.[37] showed that central section segments are less mobile than the ends due to anisotropic friction caused by entanglements with neighboring chains in the reptation regime. A higher mobility implies a higher probability of meeting functional groups attached to the ends of complementary polymers. However, we expect this effect to be small in our case since the molecular weight of the functional PMMAs is not significantly above $M_e \approx 10$ kg/mol, the entangle-

ment molecular weight of PMMA.[38] The other possible cause is steric hindrance due to the polymer chains attached to the anhydride group. Anhydride in the middle is more shielded by a backbone chain than that at the end when a bulky PMMA-NH_2 approaches in ~10 Å for reaction to occur. On the other hand, this steric hindrance would be reduced by convective flow in the mixer, which extends the chains, exposing the mid-functional groups.

Effect of the Interface on k_E/k_M. The high value of k_E/k_M at the static case indicates that the interface acts as a strong barrier against the graft copolymer formation. One explanation for this is the higher population of chain ends at the equilibrium interface than at the central segments. Helfand and Tagami predicted higher density of the chain ends at the interface by their self-consistent-field theory.[39] Zhao et al.[40] confirmed this experimentally. They reported that the density of chain ends at the interface was twice that in the bulk. In addition, polymer dynamics at the interface assists preferential segregation of the chain ends. Welp et al. reported that the chain ends started to cross the interface as soon as two surfaces of PS met and were welded, while the central segments showed a lag.[37] Thus, the interface is initially more highly populated by chain ends, producing mostly block copolymer first. A brush of diblock copolymer at the interface will slow down further reaction since new reactive polymers must diffuse through the brush.[41,42] However, this effect could be reduced by generating more fresh interface via interfacial roughening, so the conversion to PMMA-*g*-PS started to grow after 60 min, as shown in Figure 7a.

Flow Effect on the Interfacial Reaction. The interface in immiscible polymer blends during mixing is never at equilibrium due to continuous deformation, breakup, and coalescence of dispersed droplets by external flow in the mixer. The extent of deformation is greater in the early stage of mixing, i.e., less than 2 min, where the interfacial area increases by 1000 times.[43,44] As well as interfacial area change by deformation, the convection by flow will reduce the partition of the chain ends at the interface from that of the interface at equilibrium. Thus, it is expected that k_E/k_M is lowered for the interface under mixing flow. However, k_E/k_M larger than that in the homogeneous melt indicates that the effect of interface still remains. The dependence of k_E/k_M on the concentration of the functional polymer shown in Table 3 also suggests that a narrower interface favors the reaction between end-functional polymers. Russell and co-workers[45] showed that interfacial width between PS and PMMA increased from $a_I = 5$ to 8.5 nm with adsorption of block copolymer.

Interestingly, the flow applied to the heterogeneous blends had a huge influence on the interfacial reaction kinetics: $k_{E,I} = 3.2$ kg/(mol min) for the static flat interface vs 5300 kg/(mol min) for the blend-2. This influence is also found in several previous studies where reaction conversion with mixing time and morphology were reported.[21,25,46,47] Using conversion and D_{VS}, we estimated k_E and $k_{E,I}$ and summarize them in Table 4. Considering that these calculations required approximations or estimation of properties or concentrations, the k_E values are not so different from k_E in our blends and $k_{E,I} > 1000$. In addition, $k_{E,I}$ increases to 4200 kg/(mol min) for the diluted blend, PS-NH_2 (15 kg/mol)/PMMA-An (12 kg/mol) from 15 kg/(mol min) for the bilayer of PS-NH_2 (18 kg/mol)/PMMA-An (12 kg/mol). This is consistent with our observation (blend-2 vs blend-10 in Table 3).

Morphology development in immiscible polymer blends in the mixer is known to be very complex during the initial stages. Initial morphology was found to be ribbons or sheets developing to a lace structure;[43,44,48,49] thus, the interfacial area and ϕ_I at this stage could be much larger than that of the fully developed particles-in-matrix structure shown in Figure 9c. This would decrease $k_{E,I}$. Also, the effect of convection flow should be considered. It will enhance the collision probability at the interface between complementary functional polymers. Although the concentration profile at the interface is not well-known under flow, it is likely that convection would give a higher concentration of functional groups near the interface than in the case of the static interface. This convection effect should be carefully investigated further by excluding morphology change due to flow.

Before closing the discussion, it should be noted that we observed coalescence after 2 min for the blend-2 (compare parts b and c of Figure 9). This appears to be due to insufficient coverage Σ.

$$\Sigma = \frac{X_A \phi_{PS} N_{av} \rho_{PS} D_{VS}}{6 M_{n,PS}} \tag{15}$$

Σ is 0.017 chain/nm^2, which is only 10% of $\Sigma_{max} = 0.16$ chain/nm^2. According to Lyu et al.,[50,51] there exists a minimum coverage of copolymer, Σ_{min}, to suppress coalescence, and it depends on the molecular weight of the copolymer. Although our system is different from their high-density polyethylene (HDPE) and PS blend, we can apply their results to ours since coalescence will be less controlled by chemical structure than by copolymer concentration. For a 20−20 kg/mol PS-*b*-PE, they found that $\Sigma_{min} \approx \Sigma_{max}$. Thus, with Σ at 2 min coalescence could not be suppressed. Further reaction at the partially covered interface was not fast enough to prohibit coalescence by flow, and Σ at 20 min was 0.041 chains/nm^2.

Conclusions

The rate constant ratio of block copolymer and graft copolymer formation, k_E/k_M, was investigated by using phthalic anhydride end- and mid-functional PMMAs (PMMA-eAn and PMMA-mAn) and amine-terminal PMMA and PS (PMMA-NH_2 and PS-NH_2) under a competitive reaction condition. The extent of coupling to block and graft copolymers in a competitive reaction could be selectively measured by incorporating two different fluorescent groups, NBD and anthracene, to PMMA-eAn and PMMA-mAn, respectively, and by using GPC with a fluorescence detector. We have examined the effect of reaction conditions on k_E/k_M and the rate constants by observing the reaction in solution, homogeneous melt, and heterogeneous melts under static condition and under flow.

In solution, the reaction between PMMA-mAn and PS-NH_2 was slower than that with PMMA-eAn, giving $k_E/k_M = 2.8$. This result is expected from the kinetic excluded-volume effect, which theoretically predicts $k_E/k_M = 2.1$. However, even in the homogeneous melt where no kinetic excluded-volume effect is expected, $k_E/k_M = 1.7$. The deviation from theory is attributed to steric

hindrance by the polymer chain shielding a functional group at its center.

The effect of the interface on k_E/k_M was significant, resulting in $k_E/k_M > 10$. Preferential segregation of end groups due to thermodynamics as well as chain dynamics is considered as causes. When we applied flow to the heterogeneous blend, this interfacial effect was reduced. However, the effect was still observed showing a higher k_E/k_M (>2.6) than in the homogeneous melt. More importantly, we found that flow increased the rate of interfacial reaction tremendously. The interfacial rate constant in the heterogeneous blend is about 1700 times faster than at the static flat interface. This is not understood well yet. The mechanism should be investigated by observing the reaction at the interface under a controlled flow with elimination of morphology development effects that attend the use of common mixers. Such studies are under investigation.

Acknowledgment. The research was supported by grants from the Dow Chemical Co. and the MRSEC Program of the National Science Foundation under Award DMR-0212302. H.K.J. thanks Todd Jones, SuPing Lyu, and Jianbin Zhang for helpful discussions and comments. CERM is indebted to the Belgian Science Policy for financial support in the frame of the Interuniversity Attraction Poles Programme (PAI V/03).

References and Notes

(1) Flory, P. J. *Principles of Polymer Chemistry*; Cornell University Press: Ithaca, NY, 1953; p 69.
(2) Morawetz, H.; Cho, J.-R.; Gans, P. J. *Macromolecules* **1973**, *6*, 624−627.
(3) Cho, J.-R.; Morawetz, H. *Macromolecules* **1973**, *6*, 628−631.
(4) Okamoto, A.; Shimanuki, Y.; Mita, I. *Eur. Polym. J.* **1982**, *18*, 545−548.
(5) Okamoto, A.; Toyoshima, K.; Mita, I. *Eur. Polym. J.* **1983**, *19*, 341−346.
(6) Black, P. E.; Worsfold, D. J. *J. Polym. Sci., Part A: Polym. Chem. Ed.* **1981**, *19*, 1841−1846.
(7) Worsfold, D. J. *J. Polym. Sci., Part A: Polym. Chem. Ed.* **1983**, *21*, 2271−2276.
(8) Wang, Y.; Morawetz, H. *Macromolecules* **1990**, *23*, 1753−1760.
(9) Ferrari, D. F.; Baker, W. E. *J. Polym. Sci., Part A: Polym. Chem. Ed.* **1998**, *36*, 1573−1582.
(10) Orr, C. A.; Cernohous, J. J.; Guegan, P.; Hirao, A.; Jeon, H. K.; Macosko, C. W. *Polymer* **2001**, *42*, 8171−8178.
(11) Guegan, P.; Macosko, C. W.; Ishizone, T.; Hirao, A.; Nakahama, S. *Macromolecules* **1994**, *27*, 4993−4997.
(12) Orr, C. A. Ph.D. Thesis, University of Minnesota, 1997.
(13) Kramer, E. J. *Isr. J. Chem.* **1995**, *35*, 49−51.
(14) Jiao, J.; Kramer, E. J.; de Vos, S.; Moeller, M.; Koning, C. *Macromolecules* **1999**, *32*, 6261−6269.
(15) Scott, C.; Macosko, C. *J. Polym. Sci., Part B: Polym. Phys. Ed.* **1994**, *32*, 205−213.
(16) Schulze, J. S.; Cernohous, J. J.; Hirao, A.; Lodge, T. P.; Macosko, C. W. *Macromolecules* **2000**, *33*, 1191−1198.
(17) Schulze, J. S.; Moon, B.; Lodge, T. P.; Macosko, C. W. *Macromolecules* **2001**, *34*, 200−205.
(18) Yin, Z.; Koulic, C.; Pagnoulle, C.; Jerome, R. *Langmuir* **2003**, *19*, 453−457.
(19) Oyama, H. T.; Inoue, T. *Macromolecules* **2001**, *34*, 3331−3338.
(20) Oyama, H. T.; Ougizawa, T.; Inoue, T.; Weber, M.; Tamaru, K. *Macromolecules* **2001**, *34*, 7017−7024.
(21) Jones, T. D.; Schulze, J. S.; Macosko, C. W.; Lodge, T. P. *Macromolecules* **2003**, *36*, 7212−7219.
(22) Orr, C. A.; Adedeji, A.; Hirao, A.; Bates, F. S.; Macosko, C. W. *Macromolecules* **1997**, *30*, 1243−1246.
(23) Lyu, S.-P.; Cernohous, J. J.; Bates, F. S.; Macosko, C. W. *Macromolecules* **1999**, *32*, 106−110.
(24) Moon, B.; Hoye, T. R.; Macosko, C. W. *Macromolecules* **2001**, *34*, 7941−7951.
(25) Moon, B.; Hoye, T. R.; Macosko, C. W. *Polymer* **2002**, *43*, 5501−5509.
(26) George, M.; Weiss, R. G. *J. Am. Chem. Soc.* **2001**, *123*, 10393−10394.
(27) Hampe, E. M.; Rudkevich, D. M. *Chem. Commun.* **2002**, 1450−1451.
(28) Padwa, A. R.; Sasaki, Y.; Wolske, K. A.; Macosko, C. W. *J. Polym. Sci., Part A: Polym. Chem. Ed.* **1995**, *33*, 2165−2174.
(29) Maric, M.; Macosko, C. W. *Polym. Eng. Sci.* **2001**, *41*, 118−130.
(30) Moon, B. Ph.D. Thesis, University of Minnesota, 2001.
(31) Jiao, J.; Kramer, E. J.; De Vos, S.; Moller, M.; Koning, C. *Polymer* **1999**, *40*, 3585−3588.
(32) Schulze, J. S. Ph.D. Thesis, University of Minnesota, 2001.
(33) Russell, T. P.; Menelle, A.; Hamilton, W. A.; Smith, G. S.; Satija, S. K.; Majkrzak, C. F. *Macromolecules* **1991**, *24*, 5721.
(34) Macosko, C. W.; Guegan, P.; Khandpur, A. K.; Nakayama, A.; Marechal, P.; Inoue, T. *Macromolecules* **1996**, *29*, 5590−5598.
(35) Iwata, H.; Ikada, Y. *Makromol. Chem.* **1980**, *181*, 517.
(36) Khokhlov, A. R. *Makromol. Chem., Rapid Commun.* **1981**, *2*, 633−636.
(37) Welp, K. A.; Wool, R. P.; Agrawal, G.; Satija, S. K.; Pispas, S.; Mays, J. *Macromolecules* **1999**, *32*, 5127−5138.
(38) Ferry, J. D. *Viscoelastic Properties of Polymers*, 3rd ed.; John Wiley and Sons: New York, 1980; p 374.
(39) Helfand, E.; Tagami, Y. *J. Chem. Phys.* **1972**, *56*, 3592.
(40) Zhao, W.; Zhao, X.; Rafailovich, M. H.; Sokolov, J.; Composto, R. J.; Smith, S. D.; Russell, T. P.; Dozier, W. D.; Mansfield, T.; Satkowski, M. *Macromolecules* **1993**, *26*, 561−562.
(41) O'Shaughnessy, B.; Sawhney, U. *Phys. Rev. Lett.* **1996**, *76*, 3444−3447.
(42) Fredrickson, G. H. *Phys. Rev. Lett.* **1996**, *76*, 3440−3443.
(43) Scott, C. E.; Macosko, C. W. *Polym. Bull. (Berlin)* **1991**, *26*, 341−348.
(44) Scott, C. E.; Macosko, C. W. *Polymer* **1995**, *36*, 461−470.
(45) Russell, T. P.; Menelle, A.; Hamilton, W. A.; Smith, G. S.; Satija, S. K.; Majkrzak, C. F. *Macromolecules* **1991**, *24*, 5721−5726.
(46) Yin, Z.; Koulic, C.; Jeon, H. K.; Pagnoulle, C.; Macosko, C. W.; Jerome, R. *Macromolecules* **2002**, *35*, 8917−8919.
(47) Jones, T. D. Ph.D. Thesis, University of Minnesota, 2000.
(48) Sundararaj, U.; Macosko, C. W.; Rolando, R. J.; Chan, H. T. *Polym. Eng. Sci.* **1992**, *32*, 1814−1823.
(49) Sundararaj, U.; Dori, Y.; Macosko, C. W. *Polymer* **1995**, *36*, 1957−1968.
(50) Lyu, S.; Jones, T. D.; Bates, F. S.; Macosko, C. W. *Macromolecules* **2002**, *35*, 7845−7855.
(51) Lyu, S. *Macromolecules* **2003**, *36*, 10052−10055.

MA030581N